

Electronic Supporting information

Electron diffraction unveils the 2D metal-radical framework of two molecule-based magnets.

Emre Yörük, Constance Lecourt, Dominique Housset, Yuuta Izumi, Wai Li Ling, Stéphanie Kodjikian, Evgeny Tretyakov, Katsuya Inoue, Kseniya Maryunina, Cédric Desroches, Holger Klein, Dominique Luneau*

Table of contents

1. Synthesis.....	2
2. Powder X-ray diffraction.....	3
3. Electron diffraction and crystal structure	5
4. Magnetic studies.....	23
5. References	31

1. Synthesis

Materials. 2,3-Dihydroxylamino-2,3-dimethylbutane was synthesized following a previously reported procedure.^[1] 2-(2-Imidazolyl)-4,4,5,5-tetramethyl-4,5-dihydro-1*H*-imidazolyl-3-oxide-1-oxyl (NITImH) and 2-(4,5-dimethylimidazol-2-yl)-4,4,5,5-tetramethyl-4,5-dihydro-1*H*-imidazol-3-oxide-1-oxyl (NITImHMe₂) were synthesised by condensation of 2,3-dihydroxylamino-2,3-dimethylbutane with 1*H*-imidazole-2-carbaldehyde or 4,5-dimethyl-1*H*-imidazole-2-carbaldehyde as previously reported.^[2] All other chemicals and solvents were purchased as analytical grade and were used without further purification.

Synthesis of {[Mn₂(NITIm)₃]OTf}_n (1): a solution of Mn(CH₃COO)₂·4H₂O (73.2 mg, 0.30 mmol) in methanol (10 mL) was added to a solution of NITImH (100 mg, 0.448 mmol) in methanol (10 mL). The resulting green-blue solution was then put at the bottom of a test tube, and a solution of NaOTf in excess (52 mg, 0.30 mmol) in methanol (20 mL) was added on the top of this solution. A crystalline dark green powder was isolated by filtration after 5 days and washed with methanol cold on ice. Yield: 35.6 mg, 63 %. Elemental analysis agrees with compound **1** containing methanol. Elemental analysis (%): C, 40.16; H, 4.76; Mn, 11.57; N, 17.66. Calculated for C₃₂F₃H₄₆Mn₂N₁₂O₁₀S (%): C, 40.13; F, 5.95; H, 4.84; Mn, 11.47; N, 17.55; O, 16.71; S, 3.35.

Synthesis of {[Mn₂(NITImMe₂)₃]ClO₄]_n (2): a solution of Mn(CH₃COO)₂·4H₂O (73.2 mg, 0.30 mmol) in methanol (10 mL) was added to a solution of NITImHMe₂ (100 mg, 0.448 mmol) in methanol (10 mL). The resulting green-blue solution was then put at the bottom of a test tube and a solution of NaClO₄ (36.7 mg, 0.30 mmol) in methanol (20 mL) was added on the top of this solution. A crystalline dark green powder was isolated by filtration after 5 days and washed with methanol cold on ice. Yield: 98 mg, 68 %. Elemental analysis agrees with solvent free compound **2**. Elemental analysis (%): C, 44.68; H, 5.57; Mn, 11.31; N, 17.43. Calculated for C₃₆H₅₄ClMn₂N₁₂O₁₀ (%): C, 45.03; H, 5.67; Cl, 3.69; Mn, 11.44; N, 17.50; O, 16.66.

Caution! Although not encountered in these experiments, perchlorate salts are potentially explosive and as such, only a small amount of the materials should be prepared at a time and should be handled with care.

2. Powder X-ray diffraction

Powder X-ray diffraction patterns were collected with a Bruker D2 PHASER diffractometer on polycrystalline samples sonicated in cyclohexane and dropped onto silica wafers.

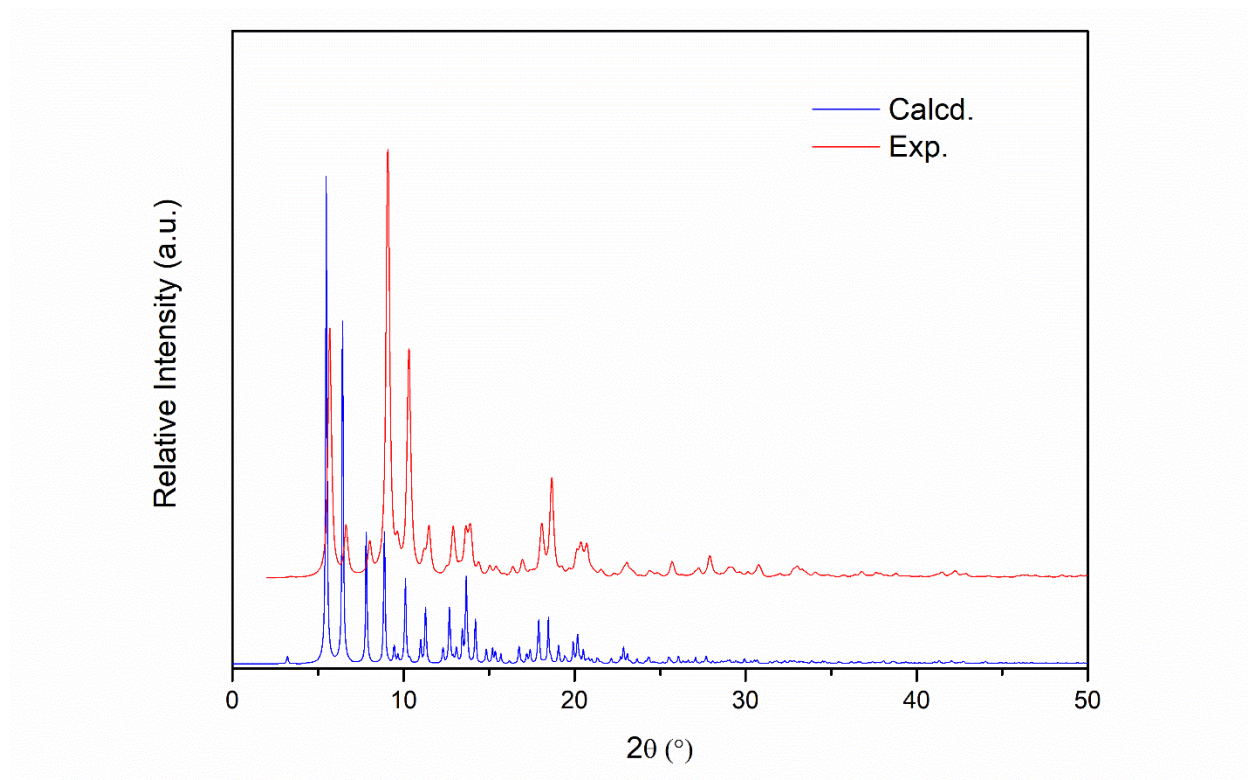


Figure S1. Experimental X-ray powder diffractogram (top: red) of compound **1** together with the calculated one (bottom: blue) from the single crystal structure at 293 K.

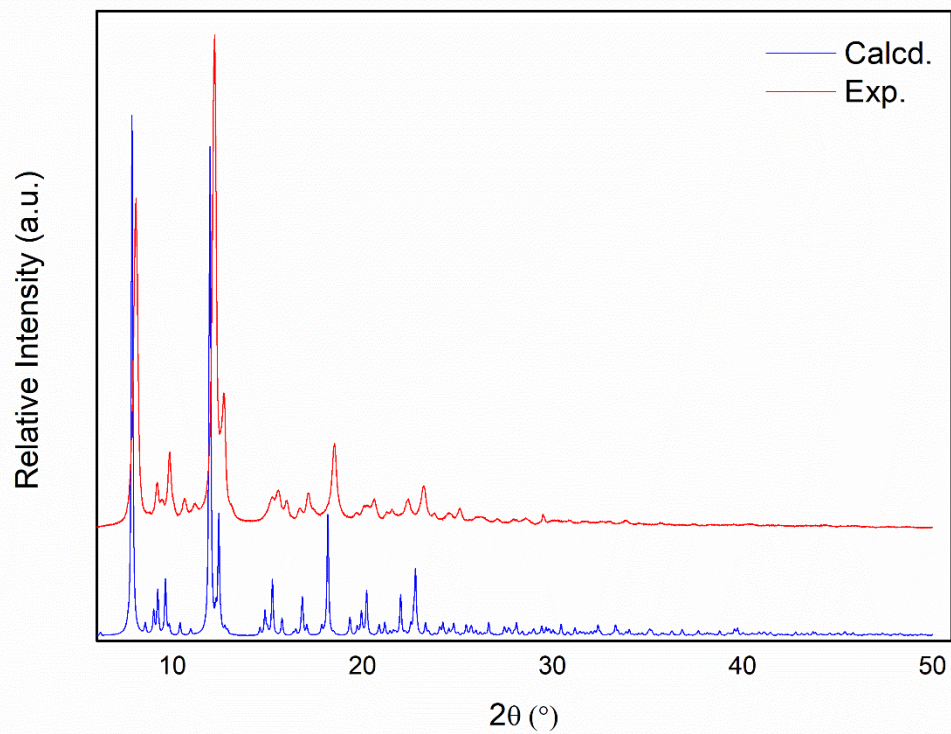


Figure S2. Experimental X-ray powder diffractogram (top: red) of compound **2** together with the calculated one (bottom: blue) from the single crystal structure at 293 K.

3. Electron diffraction and crystal structure

Data collection: The electron diffraction data were collected on a Tecnai F20 cryo-electron microscope (FEI) operated at 200 kV and equipped with a hybrid pixel Medipix3RX 512x512 detector. Samples obtained in the form of a polycrystalline powder were sonicated in cyclohexane and dropped onto a TEM grid. The diffraction data collection on different crystals was performed using the continuous rotation method with a room temperature sample holder. The speed of rotation of the compustage was set to 5% (1.47°s^{-1}) and the camera length set to 285 mm (F20 microscope settings), corresponding to a calibrated value of 505.6 mm. Data were collected with a parallel beam (C2 condenser set to 78%) with a spot size of either 5 or 6, corresponding to a dose rate on the sample of 0.029 and $0.016\text{ e}^-\text{\AA}^{-2}\cdot\text{s}^{-1}$, respectively. The dose was estimated with the F20's built-in dose monitoring device, calibrated by the Tecnai F20 manufacturer (FEI) by measuring the actual electronic current using a Faraday cup. Since this internal device was not able to monitor the very low dose settings (spot size above 6 with the F20 settings mentioned above), the Medipix3RX detector was used to estimate the dose at high spot size, by measuring the average number of counts on the entire detector surface for all spot sizes. Eight data sets from 3 different crystals were collected for $\{[\text{Mn}_2(\text{NITIm})_3]\text{OTf}\cdot\text{CH}_3\text{OH}\}_n$ (**1**), at a maximum resolution of 1.18 \AA while two data sets from a single crystal were collected for $\{[\text{Mn}_2(\text{NITImHMe}_2)_3]\text{ClO}_4\}$ (**2**), at a maximum resolution of 1.13 \AA . The diffraction data were processed and scaled with the XDS package.^[3] Data collection statistics of individual data sets are summarized in Table S1.

Structure determination and refinement: Since the resolution and the completeness of the merged data sets (Table S2) were not high enough to solve the structure by ab initio methods for both compounds, we used the molecular replacement technique, using PHASER from the CCP4 suite of programs.^[4,5] The model used is the $\{[\text{Mn}_2(\text{NITIm})_3]\text{ClO}_4\}$ structure from the Cambridge Structural Database (CSD) NUDXUF01 entry (deposition number 100351). Only two Mn^{2+} cations and three NITIm^- radical anions were kept for the search. CCDC 2330279 and 2330280 contain the supplementary crystallographic data for this paper. These data can be obtained free of charge via <https://www.ccdc.cam.ac.uk/>, or from the Cambridge Crystallographic Data Centre, 12 Union Road, Cambridge CB2 1EZ, UK; fax: (+44) 1223 336 033; or e-mail: deposit@ccdc.cam.ac.uk.

For compound **1**, the unit cell dimensions suggested us to search for two $[\text{Mn}_2(\text{NITImH})_3]$ units in the asymmetric unit. PHASER was able to place two $\text{Mn}_2(\text{NITImH})_3$ units as a highly contrasted

molecular replacement solution with a LLG of 317 (R-factor of 0.46) that was further refined with REFMAC in the kinematical approximation to an R-factor of 0.28, using the atomic electron scattering length as calculated by the Mott-Bethe formula.^[4] The inspection of the $\{2F_{\text{obs}}-F_{\text{calc}}\}$ Coulomb potential map showed a very good fit for one of the $\text{Mn}_2(\text{NITImH})_3$ entities, while the second one had only two Mn^{2+} ions and one NITIm^- anion well fitted in the $\{2F_{\text{obs}}-F_{\text{calc}}\}$ Coulomb potential map. Accordingly, the occupancy of two poorly fitted NITIm^- anions was set to zero and the refinement cycle was run again with REFMAC. The resulting $\{2F_{\text{obs}}-F_{\text{calc}}\}$ and $\{F_{\text{obs}}-F_{\text{calc}}\}$ Coulomb potential maps provided very clear indications where to place these two NITIm^- anions. These paramagnetic anions were thus moved manually with COOT in order to obtain the best possible fit with the maps,^[5] followed by another cycle of refinement with REFMAC. The R-factor improved significantly (0.23) and four Mn^{2+} ions and six NITIm^- anions fitted very well in the $\{2F_{\text{obs}}-F_{\text{calc}}\}$ Coulomb potential map. This manual placing of two NITIm^- anions was required as in the starting model the $[\text{Mn}_2(\text{NITImH})_3]$ site is in the *mer*- Δ conformation. It could thus not be superimposed onto the second $[\text{Mn}_2(\text{NITImH})_3]$ site, which is in a *fac*- Δ conformation. The full structure was ultimately refined with several cycles of manual building steps with COOT and refinement cycles with REFMAC, until no interpretable features could be found in the residual Coulomb potential map. Two triflate ions and two methanol molecules were added to the model during these steps.

For compound **2**, the structure was also solved with the $[\text{Mn}_2(\text{NITIm})_3]$ moiety of the NUDXUF01 CSD entry. Given the size of the asymmetric unit, we searched for only one $[\text{Mn}_2(\text{NITIm})_3]$ entity. The molecular replacement solution provided by PHASER was also highly contrasted, with an LLG of 133 and an R-factor of 0.44. The structure was further refined kinematically with REFMAC to an R-factor of 0.30. At that stage, the $\{2F_{\text{obs}}-F_{\text{calc}}\}$ and $\{F_{\text{obs}}-F_{\text{calc}}\}$ Coulomb potential maps clearly showed the information for missing methyl groups at the C9 and C10 position of the NITIm^- anions, confirming the presence of the NITImMe_2^- anions. Following the addition of these methyl groups, the $[\text{Mn}_2(\text{NITImMe}_2)_3]$ unit was refined to an R-factor of 0.24. Then, a perchlorate ion has been located in the $\{F_{\text{obs}}-F_{\text{calc}}\}$ Coulomb potential map and added to the model. The final model was refined to an R-factor of 0.21. The complete refinement statistics of the final models are shown in the Table S2. Refinements using the dynamical theory of diffraction were not performed due to the tremendous calculation time required for large sizes of these structures.

Table S1: data acquisition and integration statistics of individual data sets for $\{[\text{Mn}_2(\text{NITIm})_3]\text{OTf}\cdot\text{CH}_3\text{OH}\}_n$ (**1**) and $\{[\text{Mn}_2(\text{NITImMe}_2)_3]\text{ClO}_4\}_n$ (**2**).

Compound	$\{[\text{Mn}_2(\text{NITIm})_3]\text{OTf}\cdot\text{CH}_3\text{OH}\}_n$ (1)									$\{[\text{Mn}_2(\text{NITImMe}_2)_3]\text{ClO}_4\}_n$ (2)	
Data set	Crystal1-a	Crystal1-b	Crystal2-a	Crystal2-b	Crystal2-c	Crystal3-a	Crystal3-b	Crystal3-c	Crystal4-a	Crystal4-b	
Wavelength (Å)	0.02508									0.02508	
Camera length (mm)	505.60									505.60	
Exposure (s/frame)	0.50	0.50	0.25	0.25	0.25	0.25	0.25	0.25	0.25	0.25	
$\Delta\phi$ (°/frame)	0.734	0.734	0.367	0.367	0.367	0.367	0.367	0.367	0.367	0.367	
Number of frames	141	141	288	293	281	258	246	248	280	273	
Dose (e.Å ⁻²)	2.01	2.01	1.12	1.14	1.10	1.84	0.96	0.97	2.00	1.06	
Φ_{total} (°)	103.5	103.5	105.1	107.5	103.1	94.7	90.3	91.0	102.8	100.2	
Data processing											
Space group	<i>P2₁</i>									<i>P2₁2₁2₁</i>	
Unit cell dimensions (Å, °)	a=9.9 b=19.9 c=28.0 β =98.68	a=9.9 b=19.7 c=27.5 β =98.28	a=9.8 b=20.1 c=27.5 β =98.24	a=9.8 b=20.0 c=28.0 β =97.78	a=9.8 b=19.8 c=27.7 β =97.99	a=9.8 b=20.0 c=27.6 β =98.05	a=9.8 b=19.9 c=27.7 β =98.08	a=9.8 b=19.8 c=27.7 β =98.02	a=11.8 b=18.7 c=22.9	a=11.8 b=18.7 c=22.8	
Resolution (Å)	19.90 – 1.38 (1.46 – 1.38)	19.74 – 1.38 (1.46 – 1.38)	20.07 – 1.38 (1.46 – 1.38)	19.95 – 1.43 (1.51 – 1.43)	19.81 – 1.42 (1.51 – 1.42)	20.01 – 1.19 (1.26 – 1.19)	19.91 – 1.29 (1.36 – 1.29)	19.79 – 1.29 (1.37 – 1.29)	18.37 – 1.13 (1.20 – 1.13)	18.37 – 1.14 (1.21 – 1.14)	
Reflections	4733 (676)	4625 (712)	4783 (713)	4424 (627)	4199 (606)	6713 (1035)	5003 (762)	5002 (831)	7450 (1171)	7236 (1140)	
Unique reflections	1673 (247)	1644 (259)	1667 (255)	1529 (219)	1473 (215)	2231 (354)	1685 (259)	1680 (278)	1442 (230)	1357 (216)	
Completeness (%)	73.0 (70.0)	73.6 (72.8)	73.7 (73.1)	74.2 (69.7)	72.7 (69.8)	62.8 (61.6)	60.1 (58.6)	61.0 (63.2)	71.5 (71.9)	68.1 (68.40)	
R_{sym}	0.172 (0.809)	0.186 (1.442)	0.181 (0.896)	0.190 (0.980)	0.207 (1.040)	0.128 (0.996)	0.120 (1.163)	0.137 (1.452)	0.132 (0.824)	0.156 (1.335)	
R_{meas}	0.215 (1.00)	0.233 (1.803)	0.224 (1.111)	0.234 (1.200)	0.257 (1.283)	0.156 (1.221)	0.147 (1.418)	0.169 (1.759)	0.148 (0.914)	0.174 (1.475)	
$I/\sigma(I)$	3.76 (0.97)	3.57 (0.56)	3.88 (0.95)	3.61 (0.85)	3.25 (0.72)	5.11 (0.96)	5.21 (0.86)	4.65 (0.64)	7.08 (1.37)	5.85 (0.87)	
$\text{CC}_{1/2}$	0.994 (0.478)	0.995 (0.253)	0.997 (0.410)	0.996 (0.602)	0.996 (0.352)	0.998 (0.339)	0.998 (0.391)	0.998 (0.371)	0.997 (0.642)	0.996 (0.439)	

Table S2: Data statistics for merged data sets and refinement statistics. R-factor, σ bond and σ angle values correspond to the last refinement cycles made with all reflections.

	1	2	4^[6]
	<i>Electron crystallography</i>		<i>X-ray crystallography</i>
CCDC number	2330279	2330280	100351
Empirical formula	C ₃₂ H ₄₆ F ₃ Mn ₂ N ₁₂ O ₁₀ S ₁	C ₃₆ Cl ₁ H ₅₄ Mn ₂ N ₁₂ O ₁₀	C ₃₀ H ₄₂ Mn ₂ N ₁₂ O ₆ ClO ₄
Formula weight	957.73	960.22	876.09
Temperature/K	294(2)	294(2)	293(2)
Wavelength (Å)	0.02508	0.02508	0.71073
Crystal system	Monoclinic	Orthorhombic	Monoclinic
Space group	<i>P2₁</i>	<i>P2₁2₁2₁</i>	<i>P2₁</i>
a/Å	9.83	11.61	10.307(1)
b/Å	19.91	18.37	17.861(2)
c/Å	27.72	22.46	11.019(1)
β /°	98.15	90	93.638(2)
Volume/Å ³	5369.67	4790.23	2024.5(4)
Z	4	4	2
$\rho_{\text{calc}}/\text{cm}^3$	1.185	1.331	1.437
Resolution range (all. Å)	19.91–1.18 (1.21–1.18)	18.37–1.13 (1.17–1.13)	
Nb observations	39440 (437)	14640 (1313)	
Nb unique	2585 (159)	1433 (145)	
Multiplicity	15.2 (2.75)	10.2 (9.97)	
Completeness (%)	72.8 (60.2)	71.9 (72.5)	
R _{sym}	0.241 (0.984)	0.161 (1.075)	
R _{meas}	0.249 (1.209)	0.170 (1.134)	
CC _{1/2}	0.998 (0.470)	0.999 (0.715)	
I/ σ (I)	6.91 (0.86)	8.39 (1.61)	
	<i>Refinement</i>		
Resolution range (Å)	16.12 – 1.18 (1.22 – 1.18)	10.32 – 1.13 (1.16 – 1.13)	
Nb of refl. (work set)	2292 (156)	1264 (93)	
Nb of refl. (free set)	290 (11)	168 (19)	
Number of atoms	120	61	
R-factor	0.199 (0.379)	0.210 (0.328)	
R _{work}	0.200 (0.387)	0.211 (0.305)	
R _{free}	0.214 (0.330)	0.224 (0.387)	
σ bond (Å)	0.017	0.018	
σ angle (°)	2.939	3.367	
R _{sym} = R _{meas} = R-factor R _{work} = R _{free} = CC1/2 = σ bond (Å) σ angle (°)			

Table S3: Main structural features and properties within the series of compounds **1-6**.

Compounds	1	2	3	4	5	6
Reference	This work		[7]	[6]	[8]	
Formula	$[\text{Mn}^{\text{II}}_{2-y}\text{Mn}^{\text{III}}_y(\text{rad})_{3-y}(\text{red})_y]\text{X}]_n$					
Behaviour	Weak ferromagnets $y=0$ (on all temperature domain)			Valence tautomerism $y=0, 1$ or 2 (temperature-dependent)		
Radical	NITIm ⁻	NITImMe ₂ ⁻	NITBzIm ⁻	NITIm ⁻	NITIm ⁻	NITIm ⁻
Anion (X)	OTf ⁻	ClO ₄ ⁻	ClO ₄ ⁻	ClO ₄ ⁻	BF ₄ ⁻	PF ₆ ⁻
CCDC number	2330279	2330280	682014	100351	2002545	2002547
	Monoclinic	Orthorhombic		Monoclinic		
Space group	<i>P2₁</i>	<i>P2₁2₁2₁</i>		<i>P2₁</i>		
a/Å	9.83	11.61	24.62(6)	10.307(1)	10.308(3)	10.850(2)
b/Å	19.91	18.37	11.13(3)	17.861(2)	17.943(5)	17.085(4)
c/Å	27.72	22.46	18.50(5)	11.019(1)	11.085(3)	11.085(3)
β/°	98.15	90	90	93.638(2)	94.077(3)	94.362(16)
Volume/Å ³	5369.67	4790.23	5069.37	2024.5(4)	2045.1(10)	2049.0(8)
Z	4	4	4	2	2	2
ρ _{calc} /cm ³	1.185	1.331	1.345	1.437	1.402	1.432
d (Å)	13.86	11.23	12.31	10.32	10.308	10.85
Void %	21.6	6.6	18.9	6.3	7.5	6.4

d: distance between layers at room temperature with $d = c/2$ (**1, 2**); $a/2$ (**3**); a (**4-6**);

red: reduced radical

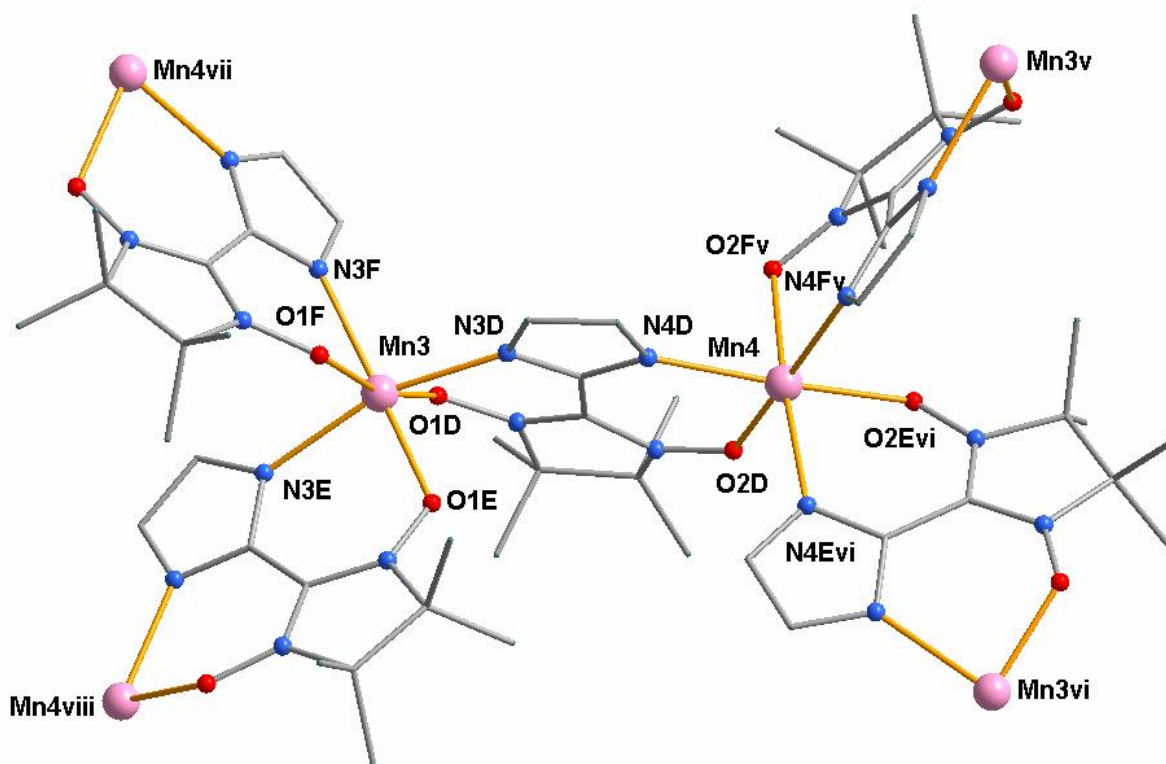


Figure S3. Figure 3. View of the second cation moiety of $[\text{Mn}^{\text{II}}_2(\text{NITIm})_3]^+$ in compound **1** showing manganese ions Mn3 and Mn4 with *fac*- Δ and *mer*- Λ conformation respectively and symmetry related atoms v : (2-x, -0.5+y, 1-z); vi : (1-x, -0.5+y, 1-z); vii : (2-x, 0.5+y, 1-z); viii : (1-x, 0.5+y, 1-z). Atoms are depicted as follows: Mn, pink; O, red; N, blue; H atoms are omitted for clarity.

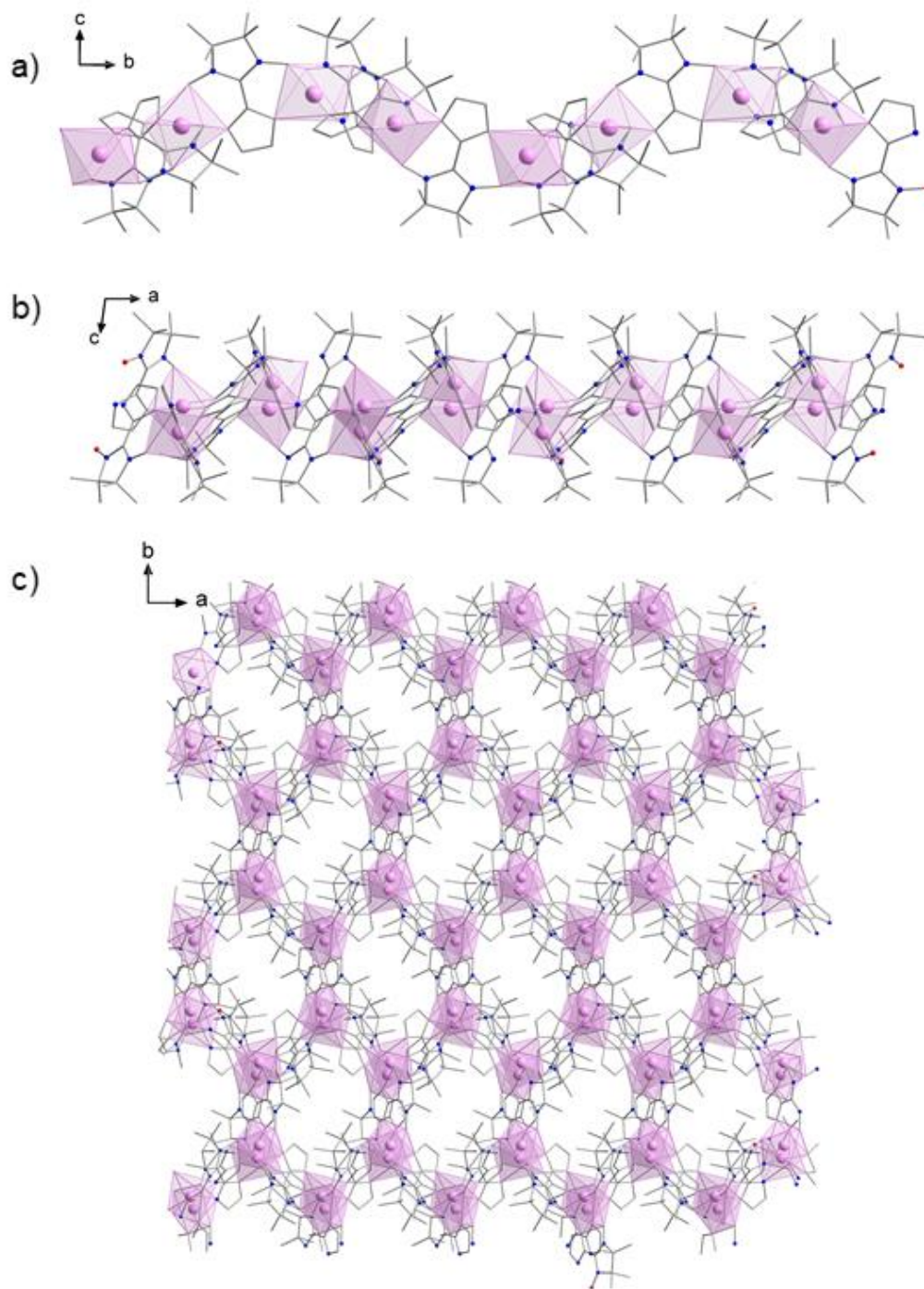


Figure S4. View of one 2D metal-radical frameworks $\{[\text{Mn}^{\text{II}}_2(\text{NITIm})_3]^+\}_n$ in compound **1** along the *a* (a), *b* (b) and *c* (c) directions. Manganese(II) ions are pink colored depicted with coordination polyhedron. Atoms are depicted as follows: Mn, pink; O, red; N, blue. Hydrogen atoms are omitted for clarity, triflate anions and inserted methanol solvent molecules are omitted for clarity.

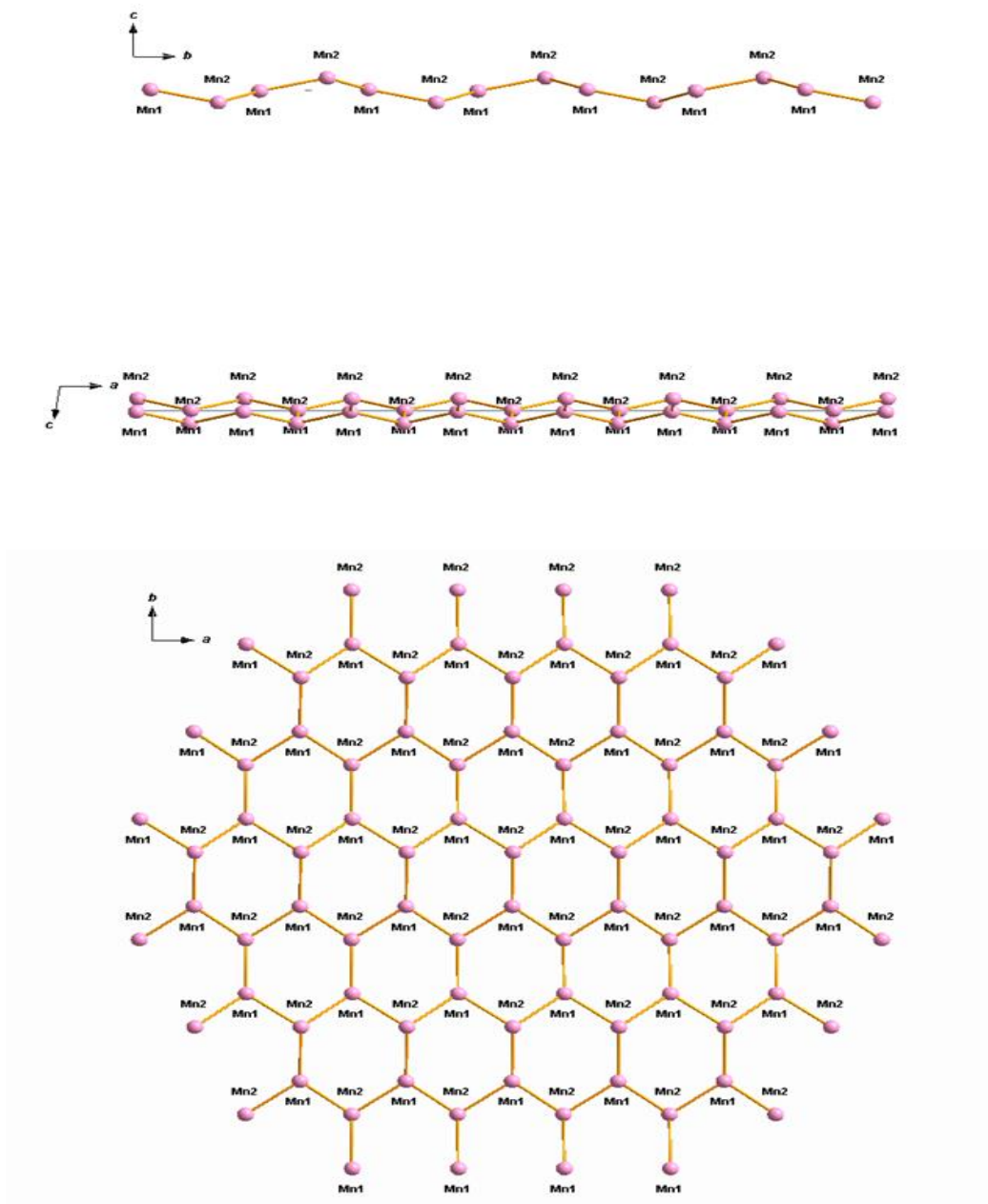


Figure S5. View showing only the 2D honeycomb-like manganese(II) network in **1** along the **a**, **b** and **c** directions (top-down). Mn^{2+} ions are pink coloured.

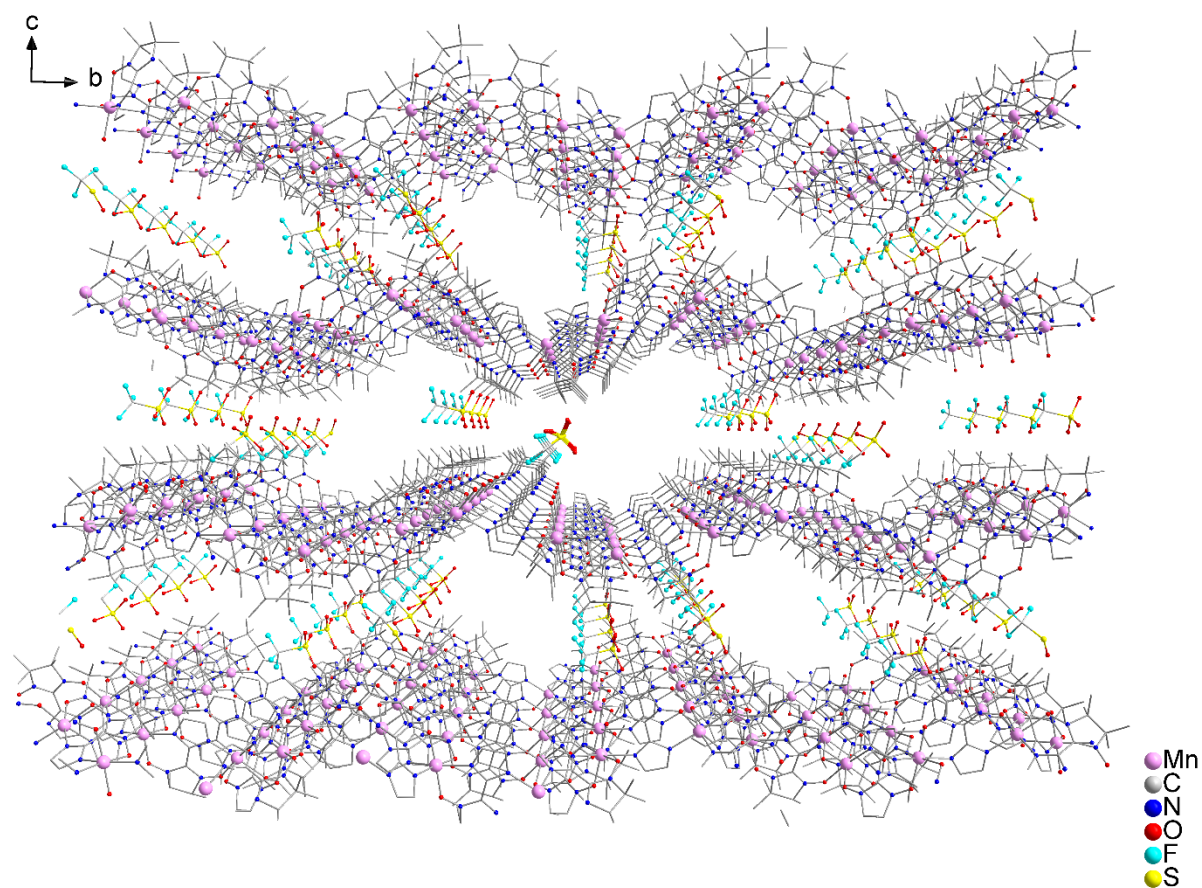


Figure S6. View of the layered structure in compound **1** along the *a* direction, showing the channels and the crest-to-through intermolecular bonding of the sheets through the triflate anions. Atoms are depicted as follows: Mn, pink; O, red; N, dark blue, S, yellow, F, light blue. Hydrogen atoms and inserted methanol solvent molecules are omitted for clarity.

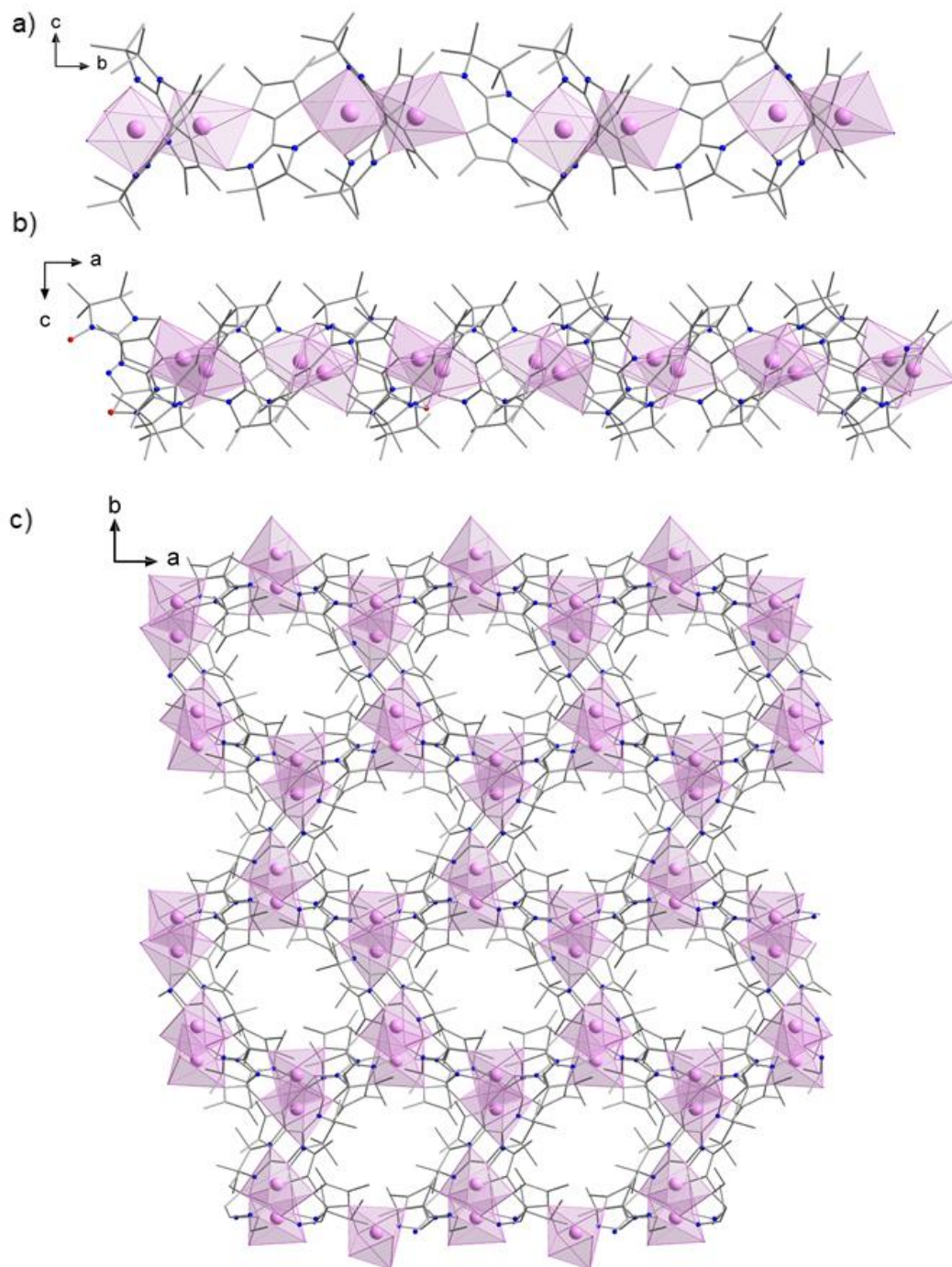


Figure S7. View of one 2D metal-radical frameworks $\{[\text{Mn}^{\text{III}}_2(\text{NITIme}_2)]^+\}_n$ along the **a** (a), **b** (b) and **c** (c) directions. Manganese(II) ions are pink colored depicted with coordination polyhedron. Atoms are depicted as follows: Mn, pink; O, red; N, blue. Hydrogen atoms and perchlorate anions are omitted for clarity.

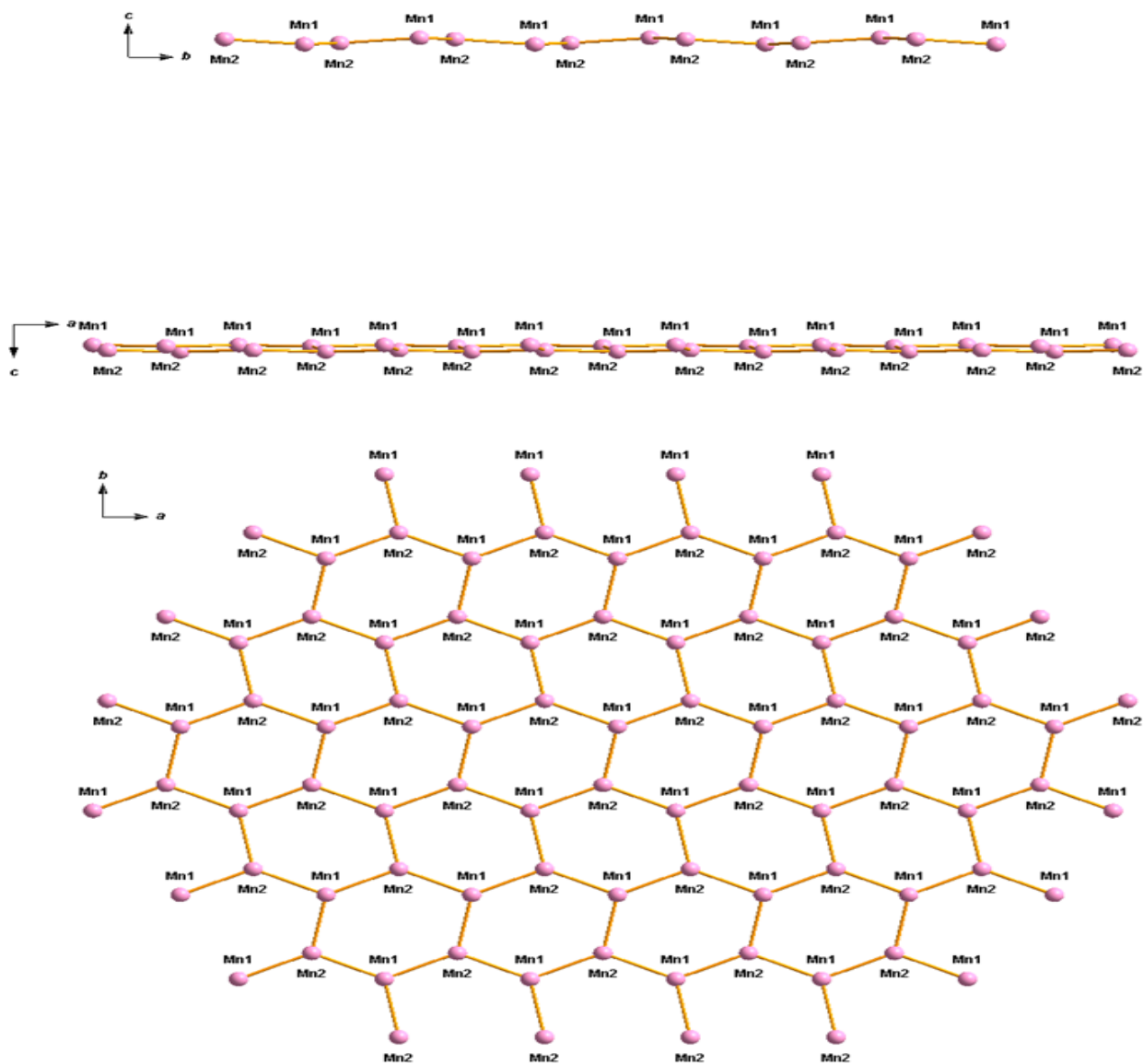


Figure S8. View showing only the 2D honeycomb-like manganese(II) network in **2** along the **a**, **b** and **c** directions (top-down). Mn^{2+} ions are pink colored.

Table S4. Selected interatomic distances (Å) for **1**.

Mn1	O1B	1.978	Mn3	O1E	2.028
Mn1	O1C	2.069	Mn3	O1D	2.145
Mn1	N3C	2.172	Mn3	N3D	2.165
Mn1	N3B	2.236	Mn3	N3F	2.236
Mn1	N3A	2.239	Mn3	N3E	2.260
Mn1	O1A	2.282	Mn3	O1F	2.296
Mn2	O2Ci	2.101	Mn4	O2D	2.148
Mn2	O2Bii	2.167	Mn4	N4Evi	2.191
Mn2	N4Bii	2.183	Mn4	O2Fv	2.198
Mn2	N4Ci	2.241	Mn4	O2Evi	2.204
Mn2	N4A	2.255	Mn4	N4D	2.222
Mn2	O2A	2.304	Mn4	N4Fv	2.222
N2A	O2A	1.313	N2D	O2D	1.321
N1A	O1A	1.327	N1D	O1D	1.341
N2B	O2B	1.319	N2E	O2E	1.330
N1B	O1B	1.345	N1E	O1E	1.321
N2C	O2C	1.302	N2F	O2F	1.314
N1C	O1C	1.341	N1F	O1F	1.326
Mn1	Mn2iv	6.312	Mn3	Mn4viii	6.309
Mn1	Mn2iii	6.338	Mn3	Mn4	6.328
Mn1	Mn2	6.396	Mn3	Mn4vii	6.373
Mn1	Mn1i	9.832	Mn3	Mn3vi	10.994
Mn1	Mn1ii	11.064	Mn3	Mn3v	11.214
Mn2	Mn1i	6.3122	Mn4	Mn3vi	6.309
Mn2	Mn1ii	6.338	Mn4	Mn3v	6.373
Mn2	Mn2iv	9.832	Mn4	Mn4vii	11.358
Mn2	Mn2iii	11.542	Mn4	Mn4viii	11.501

Symmetry relations: i: (-1+x, y, z); ii: (-x, -0.5+y, -z); iii: (-x, 0.5+y, -z); iv: (1+x, y, z); v: (2-x, -0.5+y, 1-z); vi: (1-x, -0.5+y, 1-z); vii: (2-x, 0.5+y, 1-z); viii: (1-x, 0.5+y, 1-z).

Table S5. Selected interatomic angles (°) for **1**.

O1A	Mn1	O1C	101.403	O1D	Mn3	O1E	97.456
O1A	Mn1	O1B	82.473	O1D	Mn3	O1F	166.068
O1A	Mn1	N3A	78.680	O1D	Mn3	N3D	81.873
O1A	Mn1	N3B	78.733	O1D	Mn3	N3F	88.245
O1A	Mn1	N3C	172.193	O1D	Mn3	N3E	96.954
O1B	Mn1	O1C	176.092	O1E	Mn3	O1F	94.650
O1B	Mn1	N3C	91.403	O1E	Mn3	N3D	77.591
O1B	Mn1	N3B	85.131	O1E	Mn3	N3F	174.177
O1B	Mn1	N3A	91.748	O1E	Mn3	N3E	86.183
O1C	Mn1	N3C	84.692	O1F	Mn3	N3D	94.072
O1C	Mn1	N3B	96.063	O1F	Mn3	N3F	79.548
O1C	Mn1	N3A	88.559	O1F	Mn3	N3E	90.692
N3C	Mn1	N3B	105.671	N3D	Mn3	N3F	102.170
N3C	Mn1	N3A	96.753	N3D	Mn3	N3E	163.397
N3B	Mn1	N3A	157.412	N3F	Mn3	N3E	94.330
O2A	Mn2	O2Bii	90.511	O2D	Mn4	O2Fv	84.539
O2A	Mn2	O2Ci	85.681	O2D	Mn4	O2Eiv	89.347
O2A	Mn2	N4Bii	175.759	O2D	Mn4	N4D	85.269
O2A	Mn2	N4Ci	85.918	O2D	Mn4	N4Eiv	90.532
O2A	Mn2	N4A	82.403	O2D	Mn3	N4Fv	168.161
O2B	Mn2	O2Ci	86.626	O2E	Mn4	O2Fv	87.914
O2B	Mn2	N4A	92.508	O2E	Mn4	N4D	171.226
O2B	Mn2	N4Bii	85.249	O2E	Mn4	N4Eiv	84.630
O2B	Mn2	N4Ci	172.688	O2E	Mn4	N4Fv	84.548
O2C	Mn2	N4A	168.046	O2F	Mn4	N4D	84.685
O2C	Mn2	N4Bii	93.923	O2F	Mn4	N4Eiv	171.111
O2C	Mn2	N4Ci	86.744	O2F	Mn4	N4Fv	85.109
N4A	Mn2	N4Bii	97.890	N4D	Mn4	N4Eiv	102.313
N4A	Mn2	N4Ci	93.340	N4D	Mn4	N4Fv	99.476
N4B	Mn2	N4Ci	98.280	N4E	Mn4	N4Fv	98.960

Symmetry relations: i: (-1+x, y, z); ii: (-x, -0.5+y, -z); iii: (-x, 0.5+y, -z); iv: (1+x, y, z); v: (2-x, -0.5+y, 1-z); vi: (1-x, -0.5+y, 1-z); vii: (2-x, 0.5+y, 1-z); viii: (1-x, 0.5+y, 1-z). Highlighted blue and yellow angles point to the *mer* and *fac* conformations of the ligands respectively.

Table S6. Selected interatomic distances (Å) for **2**.

Mn1	O1C	2.078	Mn2	O2Cix	1.999
Mn1	O1A	2.209	Mn2	O2Bx	2.172
Mn1	O1B	2.228	Mn2	N4Cix	2.263
Mn1	N3C	2.240	Mn2	N4Bx	2.280
Mn1	N3B	2.311	Mn2	O2A	2.295
Mn1	N3A	2.323	Mn2	N4A	2.301
O1A	N1A	1.298	O2A	N2A	1.315
O1B	N1B	1.290	O2B	N2B	1.318
O1C	N1C	1.345	O2C	N2C	1.315

Mn1	Mn2xi	6.458	Mn2	Mn1x	6.464
Mn1	Mn2xii	6.464	Mn2	Mn1ix	6.458
Mn1	Mn2	6.479	Mn2	Mn2xi	10.302
Mn1	Mn1x	10.321	Mn2	Mn2xi	11.533
Mn1	Mn1ix	11.543			

Symmetry-related atoms: ix: (-1-x, -0.5+y, -0.5-z); x : (-x, -0.5+y, -0.5-z); xi : (-1-x, 0.5+y, -0.5-z); xii : (-x, 0.5+y, -0.5-z).

Table S7. Selected interatomic angles (°) for **2**.

O1A	Mn1	O1B	86.907	O2A	Mn2	O2B	86.468
O1A	Mn1	O1C	87.797	O2A	Mn2	O2C	171.146
O1A	Mn1	N3A	76.906	O2A	Mn2	N4A	83.027
O1A	Mn1	N3B	81.206	O2A	Mn2	N4C	102.456
O1A	Mn1	N3C	172.938	O2A	Mn2	N4B	89.686
O1B	Mn1	O1C	172.048	O2C	Mn2	O2B	85.862
O1B	Mn1	N3A	87.957	O2B	Mn2	N4C	78.438
O1B	Mn1	N3B	81.568	O2B	Mn2	N4A	168.435
O1B	Mn1	N3C	100.044	O2B	Mn2	N4B	79.282
O1C	Mn1	N3C	85.416	O2C	Mn2	N4C	80.310
O1C	Mn1	N3B	103.470	O2C	Mn2	N4B	84.549
O1C	Mn1	N3A	85.068	O2C	Mn2	N4A	104.966
N3A	Mn1	N3B	156.188	N4A	Mn2	N4B	105.409
N3A	Mn1	N3C	104.400	N4A	Mn2	N4C	99.094
N3B	Mn1	N3C	98.475	N4B	Mn2	N4C	153.820

Symmetry-related atoms: ix: (-1-x, -0.5+y, -0.5-z); x : (-x, -0.5+y, -0.5-z); xi : (-1-x, 0.5+y, -0.5-z); xii : (-x, 0.5+y, -0.5-z). Highlighted blue angles point to the *mer* conformations of the ligands.

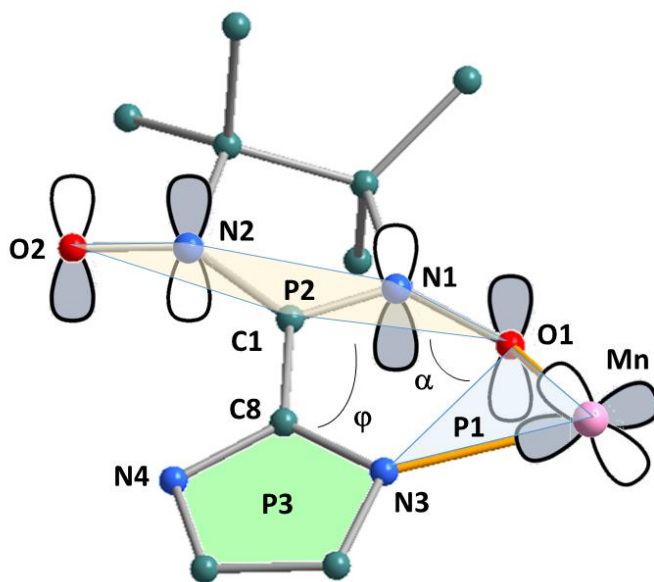


Figure S9. Scheme showing the main planes (P1, P2 and P3) and the relevant dihedral angles α and φ to consider when assessing the overlap between the metal's magnetic d orbital and the semi-occupied molecular orbital (SOMO) π^* of the nitronyl nitroxide radical.

Table S8. Dihedral angles ($^\circ$) α between P1 and P2 planes and dihedral angles ($^\circ$) φ between P2 and P3 planes for **1** as shown on Figure S9.

The asymmetric unit for **1** consists of two crystallographically independent $\{[\text{Mn}^{\text{II}}_2(\text{NITIm})_3]\text{OTf}\}$ moieties, one building around Mn1 and Mn2 and the second one around Mn3 and Mn4.

Table S8a. Dihedral angles α and φ ($^\circ$) for the Mn1 and Mn2 moiety

	P1 planes						P3 planes		
	1a	2a	3a	4a	5a	6a	10a	11a	12a
P2 planes	<i>Dihedral angle α</i>						<i>Dihedral angle φ</i>		
7a	46.005			34.774			23.355		
8a		27.584			14.10			9.307	
9a			26.068			29.023			13.633

P1 planes through coordinating atoms (O-Mn-N):Plane **1a**: O1A-Mn1-N3A; Plane **2a**: O1B-Mn1-N3B; Plane **3a**: O1C-Mn1-N3CPlane **4a**: O2A-Mn2-N4A; Plane **5a**: O2B-Mn2i-N4B; Plane **6a**: O2C-Mn2ii-N4C*i*: (-x, 0.5+y, -z); *ii*: (1+x, y, z)**P2 planes through atoms of the nitronyl nitroxide moiety (O-N-C-N-O):**Plane **7a**: O1A-N1A-C1A-N2A-O2A; Plane **8a**: O1B-N1B-C1B-N2B-O2B;Plane **9a**: O1C-N1C-C1C-N2C-O2C**P3 planes through atoms of the imidazole moiety (N-C-N):**Plane **10a**: N3A-C8A-N4A; Plane **11a**: N3B-C8B-N4B; Plane **12a**: N3C-C8C-N4C**Table S8b.** Dihedral angles α and φ ($^\circ$) for the Mn3 and Mn4 moiety

	P1 planes						P3 planes		
	1b	2b	3b	4b	5b	6b	10b	11b	12b
P2 planes	<i>Dihedral angle α</i>						<i>Dihedral angle φ</i>		
7b	31.767			12.406			8.469		
8b		34.396			28.430			15.911	
9b			34.059			37.282			17.735

P1 planes through coordinating atoms (O-Mn-N):Plane **1b**: O1D-Mn3-N3D; Plane **2b**: O2E-Mn3-N4E; Plane **3b**: O1F-Mn3-N3F;Plane **4b**: O2D-Mn4-N4D; Plane **5b**: O1E-Mn4i-N3E; Plane **6b**: O2F-Mn4ii-N3F*i*: (1-x, 0.5+z, 1-y); *ii*: (2-x, 0.5+y, 1-z)**P2 planes through atoms of the nitronyl nitroxide moiety (O-N-C-N-O):**Plane **7b**: O1D-N1D-C1D-N2D-O2D; Plane **8b**: O1E-N1E-C1E-N2E-O2E;Plane **9b**: O1F-N1F-C1F-N2F-O2F**P3 planes through atoms of the imidazole moiety (N-C-N):**Plane **10b**: N3D-C8D-N4D; Plane **11b**: N3E-C8E-N4E; Plane **12b**: N3F-C8F-N4F

Table S9. Dihedral angles ($^{\circ}$) α between P1 and P2 planes and dihedral angles ($^{\circ}$) φ between P2 and P3 planes for **2** as shown on Figure S9.

	P1 planes						P3 planes		
	1	2	3	4	5	6	10	11	12
P2 planes	Dihedral angle α						Dihedral angle φ		
7	39.151			38.104			14.377		
8		35.466			25.926			8.443	
9			13.465			3.244			6.398

P1 planes through coordinating atoms (O-Mn-N):

Plane 1: O1A-Mn1-N3A; Plane 2: O1B-Mn1-N3B; Plane 3: O1C-Mn1-N3C

Plane 4: O2A-Mn2-N4A; Plane 5: O2B-Mn2i-N4B; Plane 6: O2C-Mn2ii-N3B

i: $(-x, 0.5+y, -0.5-z)$; *ii*: $(-1-x, 0.5+y, -0.5-z)$

P2 planes through atoms of the nitronyl nitroxide moiety (O-N-C-N-O):

Plane 7: O1A-N1A-C1A-N2A-O2A;

Plane 8: O1B-N1B-C1B-N2B-O2B;

Plane 9: O1C-N1C-C1C-N2C-O2C

P3 planes through atoms of the imidazole moiety (N-C-N):

Plane 10: N3A-C8A-N4A; Plane 11: N3B-C8B-N4B; Plane 12: N3C-C8C-N4C

4. Magnetic studies

Magnetic measurements: Temperature-dependent magnetic susceptibility and magnetization isotherm data were collected on polycrystalline powder samples in polycarbonate capsules using a SQUID magnetometer (Quantum Design model MPMS-XL). All data were then corrected for the contribution of the sample holder and molecular diamagnetism estimated from Pascal's constants.^[9]

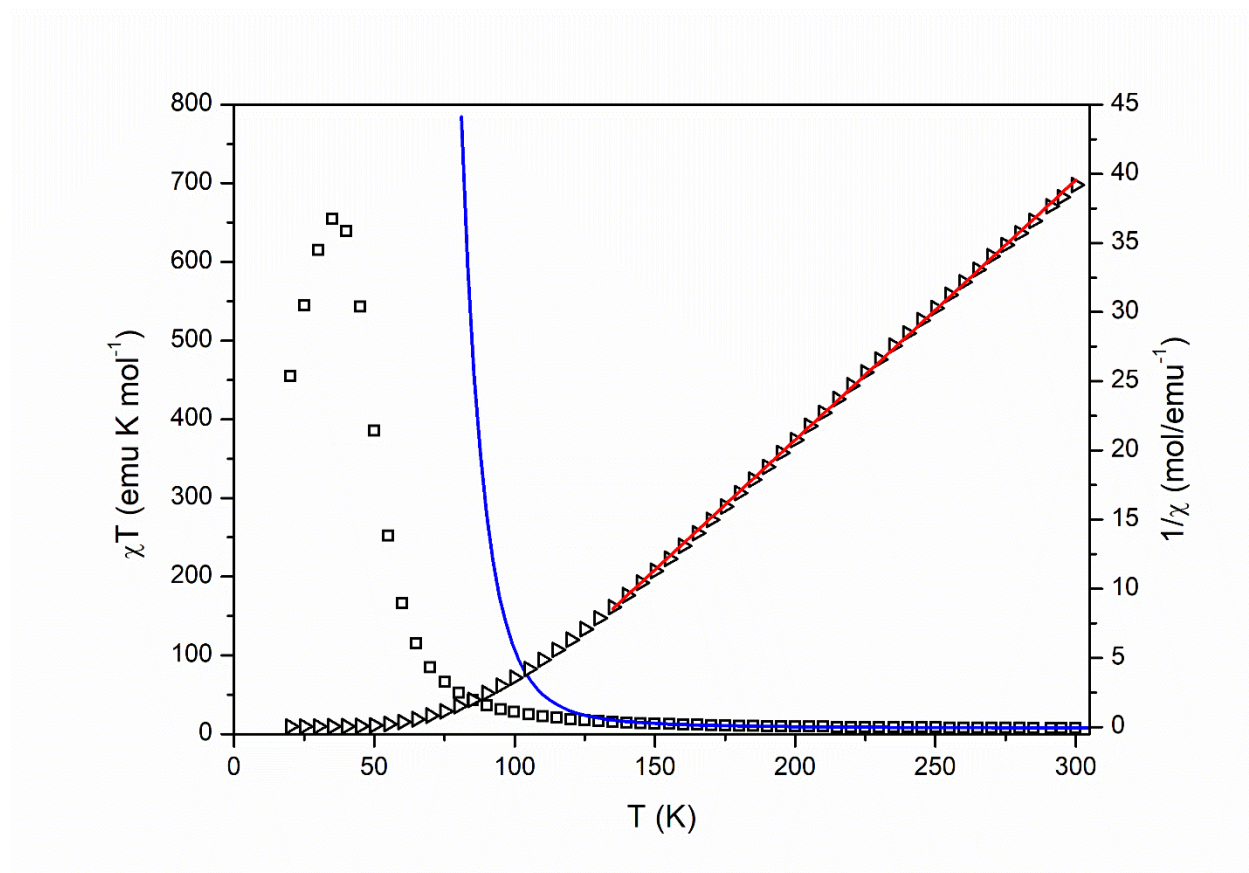


Figure S10: χT (left, squares) and $1/\chi$ (right, triangles) vs. T for $\{[\text{Mn}_2(\text{NITImMe}_2)_3]\text{ClO}_4\}_n$ (**2**) at $H = 1000$ Oe. The blue (χT) and red ($1/\chi$) solid lines represent the fit of the data as described in the text.

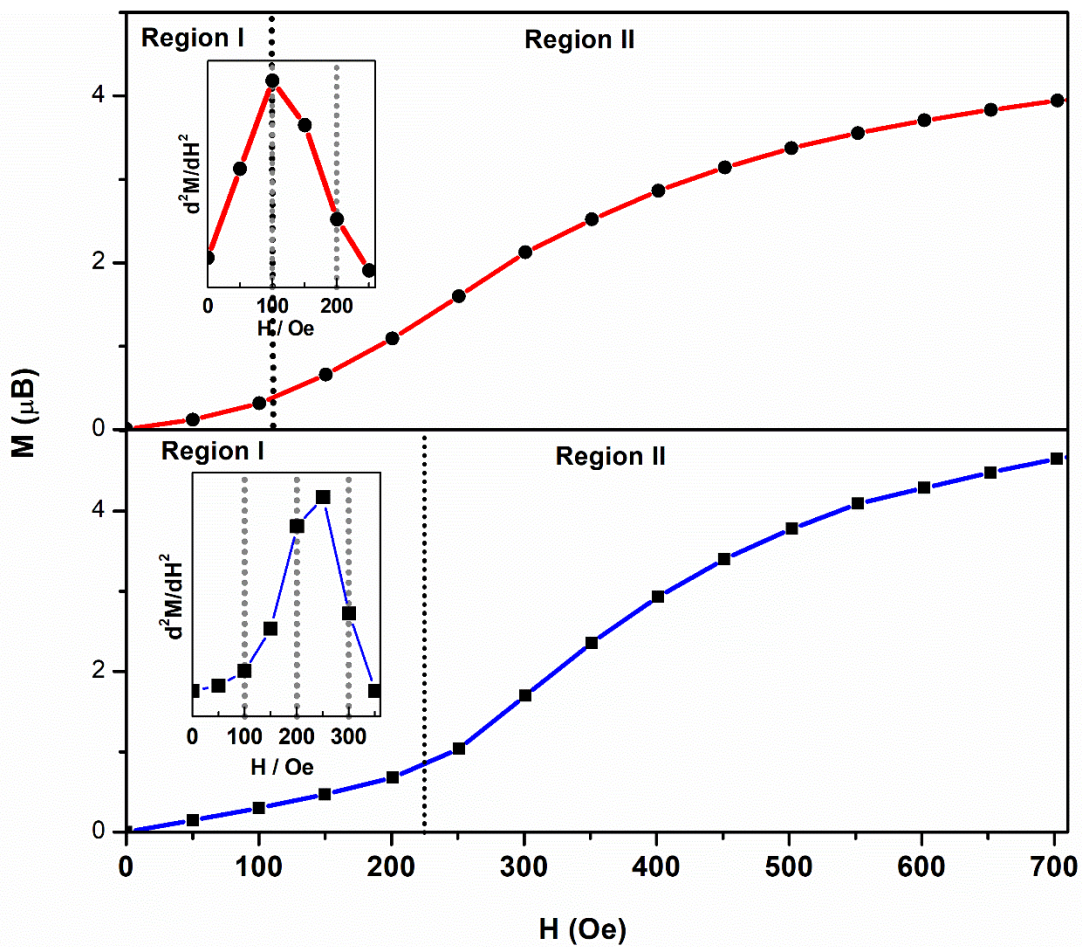


Figure S11: Field dependence of the first magnetization for **1** (bottom, squares) and for **2** (top, circles) at 2 K and low magnetic fields. The inset is the second derivative around the inflection point. The vertical dotted lines separate the linear field dependence (Region I) from the asymptotic one (Region II).

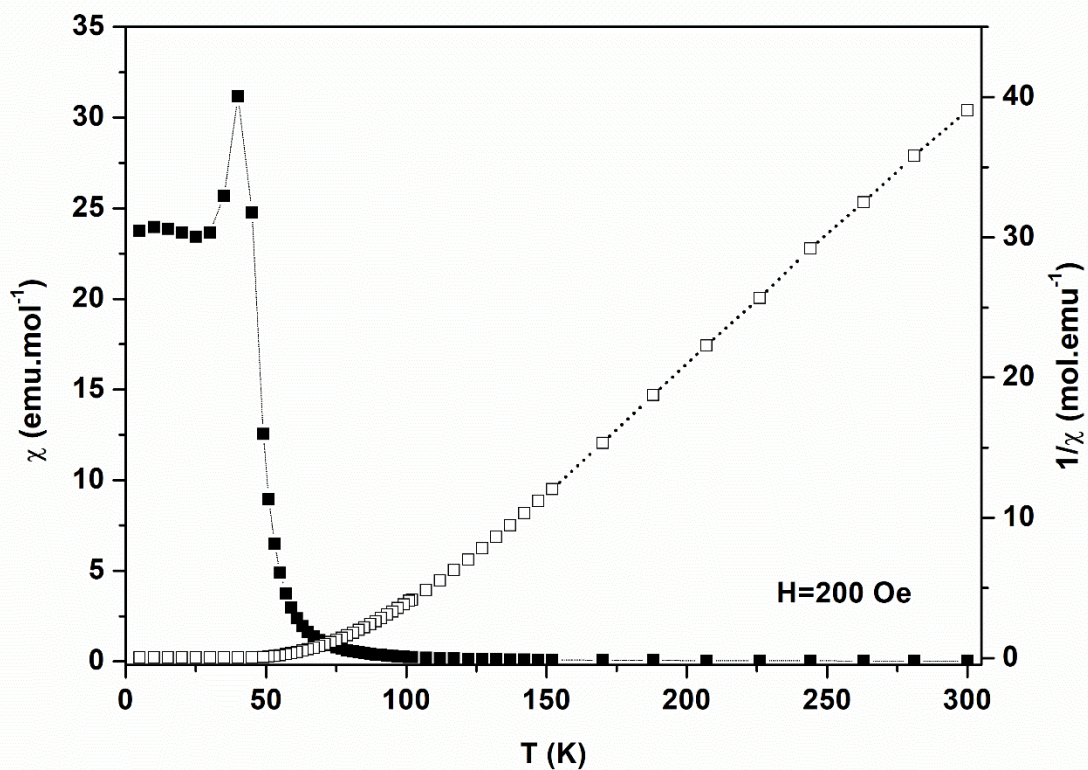


Figure S12: χ (left, plain squares) and $1/\chi$ (right, open squares) vs. T for $\{[\text{Mn}^{\text{II}}_2(\text{NITIm})_3]\text{OTf}\}_n$ (1) at $H = 200$ Oe (Region I). The dotted lines are eye guides.

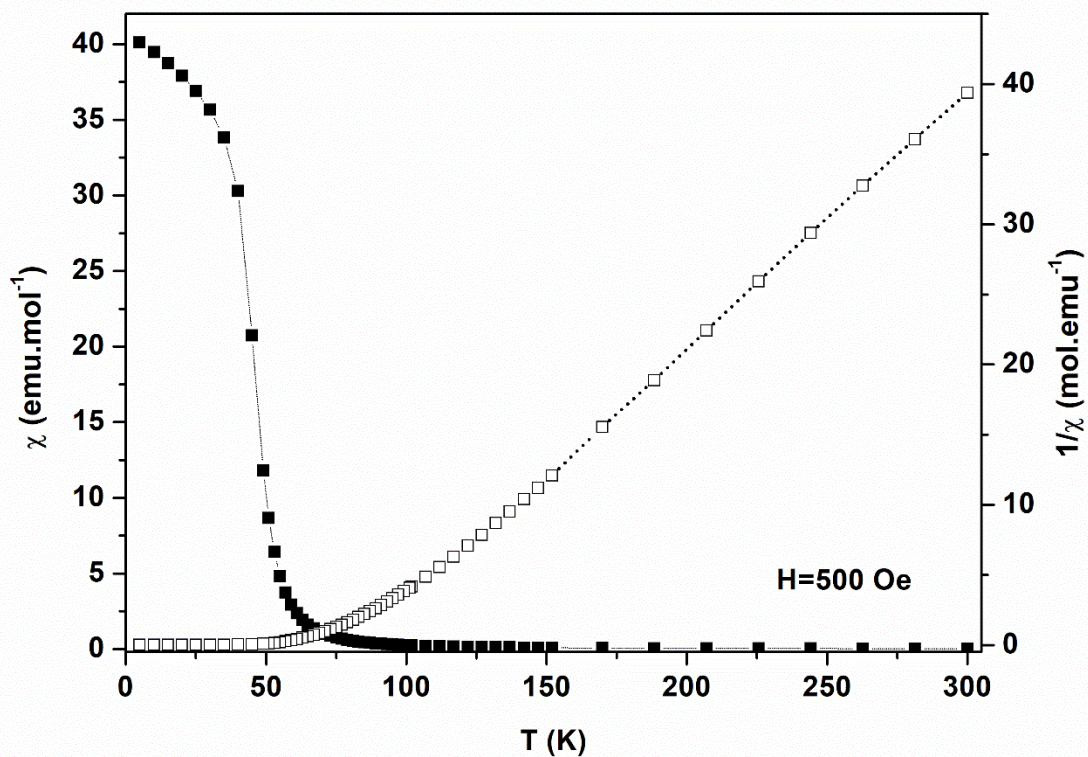


Figure S13: χ (left, plain squares) and $1/\chi$ (right, open squares) vs. T for $\{[\text{Mn}^{\text{II}}_2(\text{NITIm})_3]\text{OTf}\}_n$ (1) at H = 500 Oe (Region II). The dotted lines are eye guides.

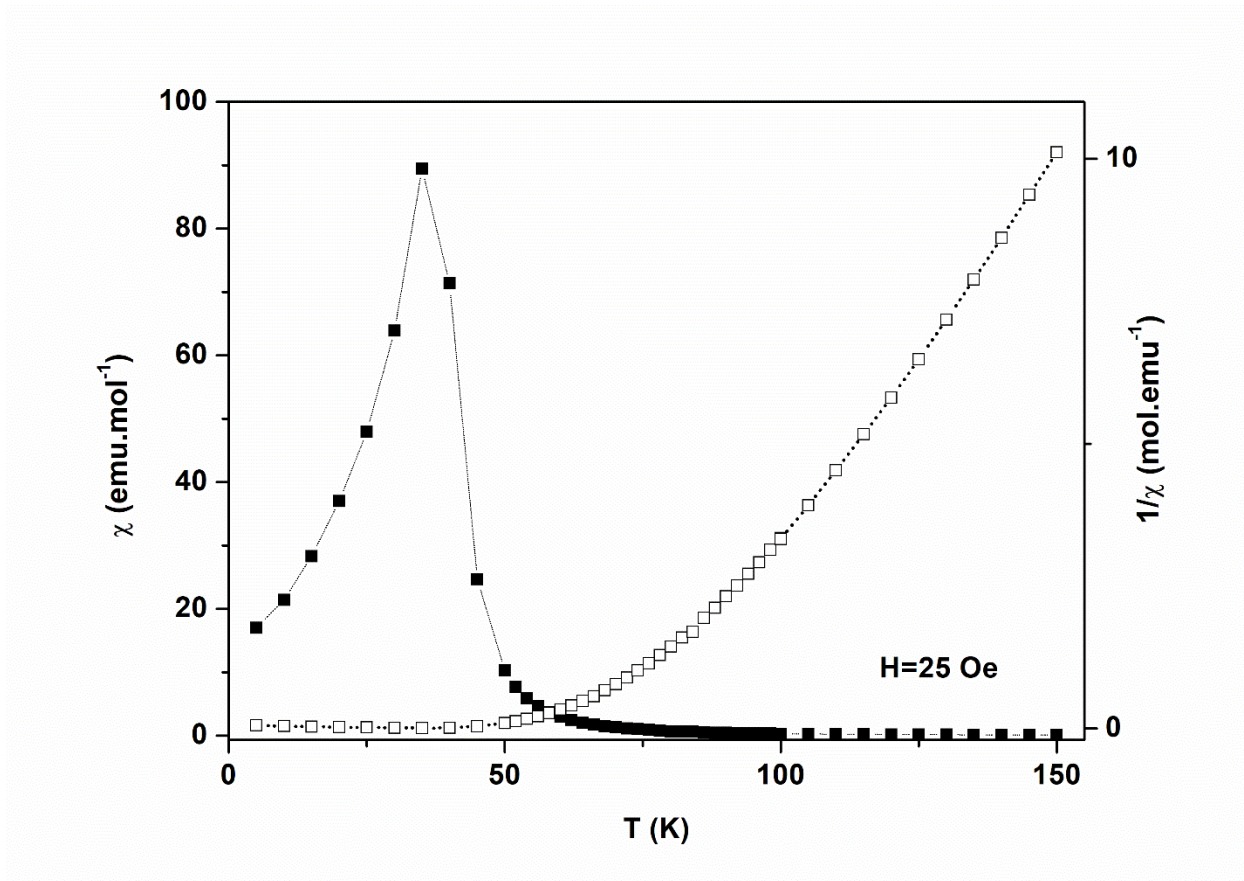


Figure S14: χ (left, plain squares) and $1/\chi$ (right, open squares) vs. T for $\{[\text{Mn}_2(\text{NITIme}_2)_3]\text{ClO}_4\}_n$ (**2**) at $H = 25$ Oe (Region I). The dotted lines are eye guides.

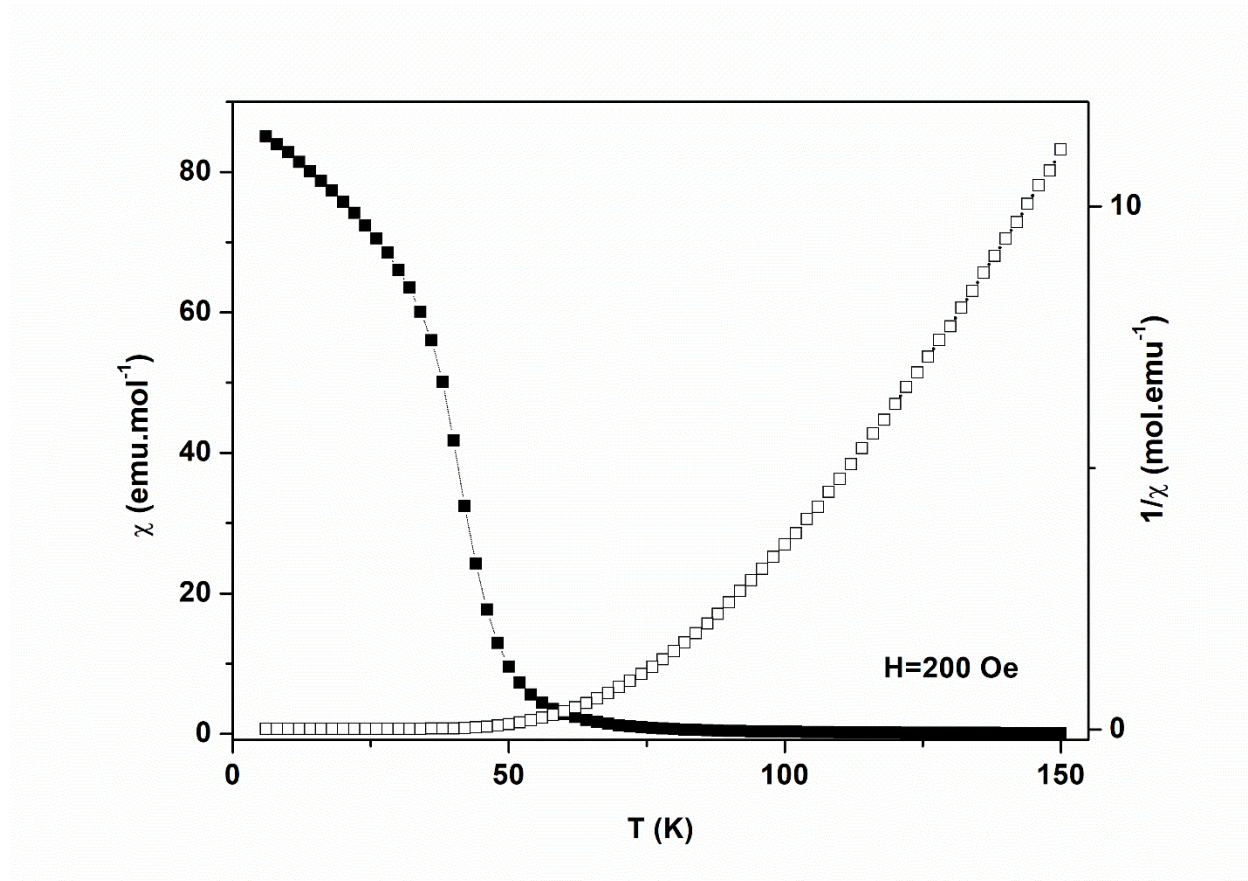


Figure S15: χ (left, plain squares) and $1/\chi$ (right, open squares) vs. T for $\{[\text{Mn}_2(\text{NITImMe}_2)_3]\text{ClO}_4\}_n$ (**2**) at $H = 200$ Oe (Region II). The dotted lines are eye guides.

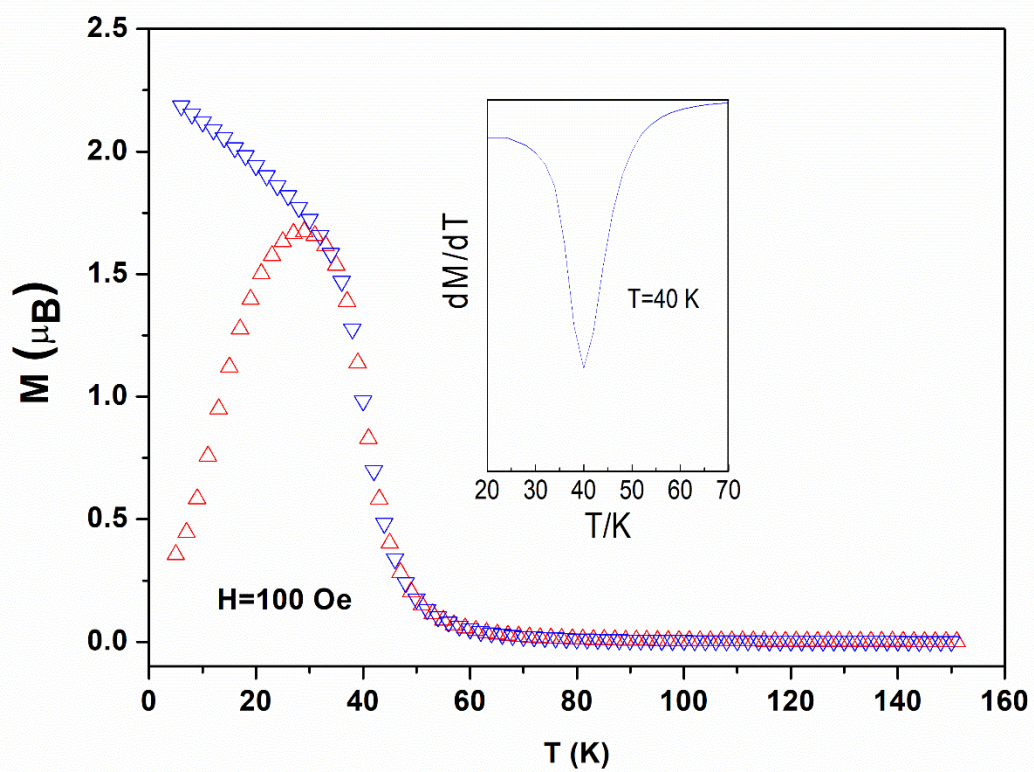


Figure S16: Zero field cool (red triangles) and field cool (blue triangles) magnetization for **2** in a magnetic field $H = 100$ Oe. The inset shows the first derivative (dM/dT) in the T_c region.

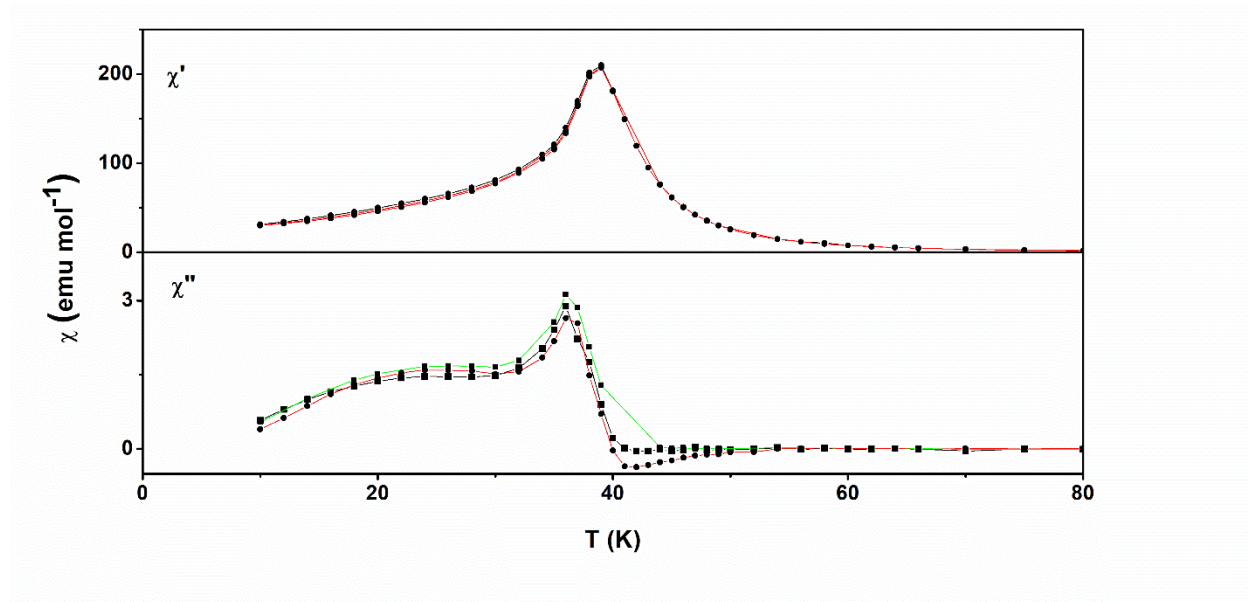


Figure S17: Temperature dependence of the in-phase and out-of-phase components of the susceptibility at AC field frequencies 10 (black), 100 (green), 500 (red), and 1400 (blue) Hz and 0 Oe applied dc field for compound **2**.

5. References

- [1] C. Hirel, K. E. Vostrikova, J. Pecaut, V. I. Ovcharenko, P. Rey, *Chem. Eur. J.* **2001**, *7*, 2007-2014.
- [2] (a) K. Fegy, D. Luneau, T. Ohm, C. Paulsen, P. Rey, *Angew. Chem. Int. Ed.* **1998**, *37*, 1270-1273; (b) V. Romanov, I. Bagryanskaya, N. Gritsan, D. Gorbunov, Y. Vlasenko, M. Yusubov, E. Zaytseva, D. Luneau, E. Tretyakov, *Crystals* **2019**, *9*, 219.
- [3] W. Kabsch, *Acta Cryst. D* **2010**, *66*, 125-132.
- [4] O. Kovalevskiy, R. A. Nicholls, F. Long, A. Carlon, G. N. Murshudov, *Acta Cryst. D* **2018**, *74*, 215-227.
- [5] P. Emsley, K. Cowtan, *Acta Cryst. D* **2004**, *60*, 2126-2132.
- [6] A. Lannes, Y. Suffren, J. B. Tommasino, R. Chiriac, F. Toche, L. Khrouz, F. Molton, C. Duboc, I. Kieffer, J. L. Hazemann, C. Reber, A. Hauser, D. Luneau, *J. Am. Chem. Soc.* **2016**, *138*, 16493-16501.
- [7] D. Luneau, A. Borta, Y. Chumakov, J.-F. Jacquot, E. Jeanneau, C. Lescop, P. Rey, *Inorg. Chim. Acta* **2008**, *361*, 3669-3676.
- [8] (a) C. Lecourt, Y. Izumi, L. Khrouz, F. Toche, R. Chiriac, N. Bélanger-Desmarais, C. Reber, O. Fabelo, K. Inoue, C. Desroches, D. Luneau, *Dalton Trans.* **2020**, *49*, 15646-15662; (b) C. Lecourt, Y. Izumi, K. Maryunina, K. Inoue, N. Belanger-Desmarais, C. Reber, C. Desroches, D. Luneau, *Chem. Commun.* **2021**, *57*, 2376-2379.
- [9] (a) O. Kahn, *Molecular Magnetism*, VCH, New York, **1993**; (b) P. Pascal, *Ann. Chim. Phys.* **1910**, *19*, 5-70.